EDGE-ENHANCING SUPER-RESOLUTION USING ANISOTROPIC DIFFUSION

Hyunwoo Kim, Jeong-Hun Jang, Ki-Sang Hong

Dept. of Electrical and Computer Engineering
POSTECH, Pohang, 790-784, Republic of Korea
{pccc,jeonghun,hongks}@postech.ac.kr

ABSTRACT

This paper presents an edge-enhancing super-resolution algorithm using anisotropic diffusion technique. Because we solve the super-resolution problem by incorporating anisotropic diffusion, our technique does more than merely reconstruct a high-resolution image from several overlapping noisy low-resolution images and preserve them. In addition to reducing image noise during the restoration process, our method also enhances edges. We apply this technique to a video stream which can be aligned by 3x3 projective transformations.

1. INTRODUCTION

Image resolution/quality is limited to the characteristic of imaging sensors and/or image degradation due to lossy compression. Recently, to overcome resolution limitations due to imaging degradation, researchers have tried to reconstruct a high-resolution image from a collection of noisy low resolution images, called *super-resolution*.

In this paper, we focus our attention on the super-resolution of 2D scenes, which can be approximated by a planar image (i.e., when videos are captured from planar objects or far away scenes or obtained by rotating and zooming cameras). All frames from a 2D scene can be aligned to a single frame. This results in a compact video representation called an *image mosaic*. Since the motion estimation in videos from 2D scenes is easy and accurate compared to that of general videos and it can be extended to general videos at the cost of difficult motion estimation, many algorithms have been developed and experimented with videos from 2D scenes.

Many researchers have tried to improve super-resolution performance by developing many restoration algorithms. To restore a super-resolved image from a 2D video, Irani and Peleg [4, 5] introduced an iterative back-projection algorithm, which ensures convergence while suppressing spurious noise components in the solution, owing to the proper selection of a back-projection function. Man and Picard [7] extended this to the projective case and Zomet and Peleg [9] rendered the original implementation more efficient, and applied it to image mosaics. In order to preserve edge information while removing image noise, many algorithms have been developed. In particular, Elad and Feuer [3] introduced the super-resolution problem as a generalizion of single image restoration and they developed several ML and MAP estimtors. Capel and Zisserman [1, 2] investigated an ML estimator, a MAP estimator based on Huber prior, and an estimator, which was regularized using the Total Variation norm for the super-resolution of image mosaics and text images.

However, when a target image includes edges/lines, as shown in Figures 1(a), they can be easily aliased in low-resolution images through the imaging process. Therefore, to reduce the aliasing artifact, we need *enhance* the structures while *preserving* them and reducing image noise. In this paper, we introduce edge-enhancing super-resolution by incorporating anisotropic diffusion. Our technique not only reconstructs a high-resolution image from several overlapping noisy low-resolution images, but also enhances edges/lines while reducing image noise during the restoration process.

Degradation modeling is explained in Section 2 and motion estimation is explained in Section 3. In Section 4, a basic super-resolution restoration formulation and its solution, called Irani-Peleg estimator, are reviewed. In Section 5, our proposed algorithm is introduced. Experimental results are given in Section 6 and concluding remarks are given in Section 7.

2. DEGRADATION MODELING

The imaging process in videos from 2D scenes can be modelled by geometric warping, blurring, sampling, and uncorrelated additive Gaussian noises added to the observed images. Elad and Feuer [3] introduced a matrix-vector formulation. Given N low-resolution images $Y_1, \cdots, Y_N$, the imaging process of Y_k from the super-resolved image X can be formulated by

$$\vec{\mathbf{y}}_k = \mathbf{D}_k \mathbf{C}_k \mathbf{F}_k \vec{\mathbf{x}} + \vec{\mathbf{e}}_k, \qquad (1)$$

where $\vec{\mathbf{x}}$ denotes a high-resolution X of size $[L \times L]$, reordered in a vector of size $[L^2]$. $\vec{\mathbf{y}}_k$ and $\vec{\mathbf{e}}_k$ denotes the

0-7803-6725-1/01/$10.00 ©2001 IEEE

kth low-resolution input image Y_k and the corresponding normally distributed additive noise of size $[M_k \times M_k]$, reordered in a vector of size $[M_k^2]$, respectively. $\mathbf{F}_k$, $\mathbf{C}_k$, and $\mathbf{D}_k$ is the geometric warp matrix, the blurring matrix, and the decimation matrix, respectively. By considering all the frames and by stacking the vector equations, we obtain a matrix-vector formula:

$$\begin{bmatrix} \vec{\mathbf{y}}_1 \\ \vdots \\ \vec{\mathbf{y}}_N \end{bmatrix} = \begin{bmatrix} \mathbf{D}_1\mathbf{C}_1\mathbf{F}_1 \\ \vdots \\ \mathbf{D}_N\mathbf{C}_N\mathbf{F}_N \end{bmatrix} \vec{\mathbf{x}} + \begin{bmatrix} \vec{\mathbf{e}}_1 \\ \vdots \\ \vec{\mathbf{e}}_N \end{bmatrix}, \tag{2}$$

which can be also represented by

$$\vec{\mathbf{y}} = \mathbf{A}\vec{\mathbf{x}} + \vec{\mathbf{e}}. \tag{3}$$

3. MOTION ESTIMATION

Kim *et al.* [6] introduced a robust, accurate global registration algorithm in the presence of moving objects. When pairwise local registrations are performed, severe global misalignment may result: errors may accumulate during the process of recovering projective transformations between two pairs of consecutive frames and concatenating the transformations to align frames into an image mosaic. To overcome the problem, a robust global registration technique is adopted, which uses a graph to represent temporal and spatial connectivity among multi-frame images. The framework presented in the paper allows the automatic construction of the graph and the construction of a consistent mosaic from a collection of multi-frame images, which works well even in the presence of moving objects. As a result, the algorithm gives accurate geometric warping matrices $\{\mathbf{F}_1, \cdots, \mathbf{F}_N\}$.

4. RESTORATION ALGORITHM

In this section we review the super resolution work of Irani *et al.* [4, 5, 9]. Assuming that the noise process is uncorrelated and has a uniform variance in all observed images in Equation (3), the maximum likelihood solution of a high-resolution image, $\vec{\mathbf{x}}$, can be estimated by minimizing the functional:

$$E(\vec{\mathbf{x}}) = \frac{1}{2}\|\vec{\mathbf{y}} - \mathbf{A}\vec{\mathbf{x}}\|^2. \tag{4}$$

The minimum of the functional occurs where the gradient of the functional is zero ($\nabla E = 0$). It is represented by

$$\nabla E = 0 \Longleftrightarrow \mathbf{A}^T(\mathbf{A}\vec{\mathbf{x}} - \vec{\mathbf{y}}) = 0$$
$$\Longleftrightarrow \sum_{k=1}^{N} \mathbf{F}_k^T\mathbf{C}_k^T\mathbf{D}_k^T(\mathbf{D}_k\mathbf{C}_k\mathbf{F}_k\vec{\mathbf{x}} - \vec{\mathbf{y}}_k) = 0. \tag{5}$$

Zomet and Peleg [9] mentioned that the multiplication with $\mathbf{A}$ and $\mathbf{A}^T\mathbf{A}$ can be implemented using only image operations, such as warp, blur, and sampling. The matrix $\mathbf{A}^T\mathbf{A}$ operating on the vector $\vec{\mathbf{x}}$ and the matrix $\mathbf{A}^T$ operating on the vector $\vec{\mathbf{y}}$ can be represented by the following image operations.

$$\begin{aligned} \mathbf{A}^T\mathbf{A}\vec{\mathbf{x}} &= \sum_{k=1}^{N} \mathbf{F}_k^T\mathbf{C}_k^T\mathbf{D}_k^T\mathbf{D}_k\mathbf{C}_k\mathbf{F}_k\vec{\mathbf{x}}, \\ \mathbf{A}^T\vec{\mathbf{y}} &= \sum_{k=1}^{N} \mathbf{F}_k^T\mathbf{C}_k^T\mathbf{D}_k^T\vec{\mathbf{y}}_k, \end{aligned} \tag{6}$$

where $\mathbf{F}_k$, $\mathbf{C}_k$, and $\mathbf{D}_k$ is implemented by image warping, blurring, and subsampling, respectively. The matrix $\mathbf{D}_k^T$ corresponds to upsampling the image. The matrix $\mathbf{C}_k^T$ is implemented by convolution with the flipped kernel for a convolution blur and $\mathbf{F}_k^T$ is forward warping of the inverse motion, if $\mathbf{F}_k$ represents backward warping.

Finally, to solve Equation (3), the authors used Richardson iterations with an iteration step:

$$\begin{aligned} \vec{\mathbf{x}}^{(n+1)} &= \vec{\mathbf{x}}^{(n)} - \nabla E \\ &= \vec{\mathbf{x}}^{(n)} + \sum_{k=1}^{N} \mathbf{F}_k^T\mathbf{C}_k^T\mathbf{D}_k^T(\vec{\mathbf{y}}_k - \mathbf{D}_k\mathbf{C}_k\mathbf{F}_k\vec{\mathbf{x}}), \end{aligned} \tag{7}$$

where $\vec{\mathbf{x}}^{(n)}$ denotes the estimate at the nth iteration with $\vec{\mathbf{x}}^{(0)}$ corresponding to the average value of all aligned images in the domain of the super-resolution solution X. This algorithm is called the *iterative backprojection algorithm* or the *Irani-Peleg estimator*.

5. SUPER-RESOLUTION WITH ANISOTROPIC DIFFUSION

Our proposed restoration algorithm incorporates an edge-enhancing anisotropic diffusion, so it not only reconstructs a high-resolution image from several overlapping noisy low-resolution images, but also enhances edges and preserves them, while reducing image noise during restoration process.

5.1. Anisotropic Nonlinear Diffusion

Diffusion is a physical process that equilibrates concentration differences without creating or destroying mass. The diffusion process is expressed by the diffusion equation:

$$\frac{\partial X}{\partial t} = \nabla \cdot \mathbf{D}\nabla X, \tag{8}$$

where X denotes concentration and $\mathbf{D}$ denotes the diffusion tensor, a positive-definite symmetric matrix. In image processing, nonlinear diffusion filters regard the original input image as the initial state of a diffusion process that adapts itself to the evolving image. The fact that nonlinear adaptation may enhance interesting structures, such as edges, relates them to image enhancement and image restoration methods [8]. The design of the nonlinear diffusion filters may be reduced to design the diffusion tensor

$\mathbf{D}$ and the tensor is closely related to the differential structure of the evolving image. We are particularly interested in anisotropic cases where $\mathbf{D}\nabla X$ and ∇X are not parallel.

5.2. Incorporating Anisotropic Diffusion

By using an image representation instead of a matrix-vector representation and adding a regularization functional $T(|\nabla X|^2)$, Equation (4) can be rewritten, in a continuous form, by

$$\begin{aligned} E(X) &= \int\int_R [\, \frac{1}{N}\sum_{k=1}^{N}\{Y_k(x,y) - a_k(X)(x,y)\}^2 \\ &+ \gamma T(|\nabla X|^2)\,]\,dxdy. \end{aligned} \tag{9}$$

where $a_k(X)$ is the transformed image of the super-resolution image X with the image operation corresponding to $\mathbf{A}_k$ (=$\mathbf{D}_k\mathbf{C}_k\mathbf{F}_k$) and Y_k is the kth input image. In this case, the corresponding gradient descent equation is represented by

$$\frac{\partial X}{\partial t} = \sum_{k=1}^{N}\{a_k^T(Y_k) - a_k^T a_k(X)\} + \gamma N\nabla\cdot\dot{T}(|\nabla X|^2)\nabla X \tag{10}$$

where $a_k^T a_k(X)$ is the transformed image of the super-resolution image X, with the image operations corresponding to the matrix $\mathbf{A}_k^T\mathbf{A}_k$, and $a_k^T(Y_k)$ is the transformed image of Y_k, with the image operations corresponding to the matrix $\mathbf{A}_k^T$.

Specifying $\dot{T}(|\nabla X|^2)$ with $1/(1+|\nabla X|^2/\lambda^2)$ called Perona-Malik diffusion [8], we can reconstruct a super-resolution image from low-resolution images, and remove image noise while preserving edges during the restoration process. We term the method *edge-preserving super-resolution* and and it is used in our experiments to compare the following proposed edge-enhancing regularization with general edge-preserving regularizations.

5.3. Edge-Enhancing Super-Resolution

In order to enhance edge structure, the diffusion term not only takes into account the contrast of an edge, but also its direction during the evolution process [8]. To incorporate the characteristic of edge-enhancing anisotropic diffusion into super-resolution, the scalar $\dot{T}(|\nabla X|^2)$ may be replaced with the 2x2 diffusion tensor $\mathbf{D}$ as follows. When we define $D(|\nabla X_\sigma|^2) \equiv 1/(1+|\nabla X|^2/\lambda^2)$, Equation (10) can be rewritten by

$$\frac{\partial X}{\partial t} = \sum_{k=1}^{N}\{a_k^T(Y_k) - a_k^T a_k(X)\} + \gamma N\nabla\cdot\mathbf{D}\nabla X, \tag{11}$$

where

$$\mathbf{D} = \begin{bmatrix}\mathbf{v}_1 & \mathbf{v}_2\end{bmatrix}\begin{bmatrix}D(|\nabla X_\sigma|^2) & 0 \\ 0 & 1\end{bmatrix}\begin{bmatrix}\mathbf{v}_1^T \\ \mathbf{v}_2^T\end{bmatrix} \tag{12}$$

such that $\mathbf{v}_1 \parallel \nabla X_\sigma$ and $\mathbf{v}_2 \perp \nabla X_\sigma$. In this equation, ∇X_σ denotes the gradient of the Gaussian-convolved image $(K_\sigma * X)$ with scale σ and it is insensitive to structures with scales smaller than σ. In smooth regions, since $D(|\nabla X_\sigma|^2)$ is close to 1, $\mathbf{D}\nabla X \approx \{\mathbf{v}_1\mathbf{v}_1^T + \mathbf{v}_2\mathbf{v}_2^T\}\nabla X$ and it means the regions are smoothed in all directions. In edge regions, since $D(|\nabla X_\sigma|^2)$ is close to 0, $\mathbf{D}_{EE}\nabla X \approx \mathbf{v}_2\mathbf{v}_2^T\nabla X$. Therefore, edges are smoothed only in the edge direction $\mathbf{v}_2$ and this results in edge enhancement in the restoration process. (Notice that $\mathbf{v}_1$ and $\mathbf{v}_2$ is perpendicular and parallel to an edge.) By using the functional, we can enhance edges while reducing noise during the evolution process. This is called *edge-enhancing super-resolution*.

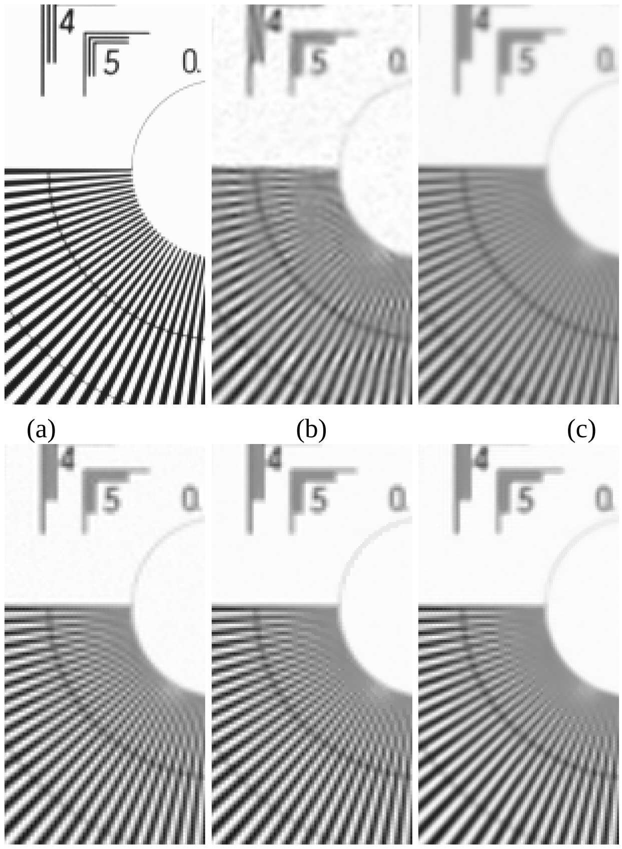

(a) (b) (c) (d) (e) (f)

Fig. 1. Simulation result (2x2 Enlargement). (a) A original chart image (100x200) (b) Bi-cubic interpolation of a low-resolution frame, (c) Average blending, (d) Irani-Peleg estimator, (e) Edge-preserving super-resolution, (f) Edge-enhancing super-resolution ($\sigma = 0.5, \lambda = 3.0, \gamma = 0.2$).

6. EXPERIMENTAL RESULTS

We present two experimental results. The first experiment is applied to simulated images and the other is applied to a real video. First, we obtain simulated low-resolution images from the chart image shown in Figure 1(a), which contains narrow lines that may be easily aliased during the imaging process. To obtain low resolution images from the chart image, the original image is first warped with transformation parameters ($\mathbf{F}_k$) with 10 different rotations and translations, smoothed with a Gaussian filter with scale 0.8 ($\mathbf{C}_k$), 2x2 downsampled ($\mathbf{D}_k$), and added Gaussian noise with standard deviation 5.0 graylevel ($\vec{\mathbf{e}}_k$). As a result, we get 10 low-resolution images. Note that since the known warping parameters are used for our restoration process, there is no warping error in this simulation. Figures 1(b)-(f) show the super-resolved images mentioned in the caption. In the diagonal lines of the fan-shaped pattern, one observes that the recovery of the proposed edge-enhancing method is better than others as compared with the original image. The edge-preserving super-resolution results in aliased diagonal lines because the lines are aliased during the simulated imaging process and the algorithm is inherently based on an edge preserving regularization. However, our edge-enhancing method overcomes edge aliasing by smoothing line boundaries (i.e., edge enhancing).

Second, eight images are captured using a hand-held camera. Figure 2 shows a reference frame from the images. The other frames are aligned into the frame using motion estimation. Figures 3(a)-(e) show the super-resolved images as mentioned in the caption. We can see that the super-resolution algorithms restore degraded details compared with the result of bi-cubic interpolation of a low-resolution image. Moreover, we can deblur image blurring due to image mis-alignment in average blending. While the edge-preserving algorithm removes image noises in smooth regions while keeping a ringing artifact around edge boundaries, our edge-enhancing algorithm removes the ringing artifact by enhancing edges and restores degraded details simultaneously.

7. CONCLUSIONS

In this paper, we introduced an edge-enhancing super-resolution algorithm using anisotropic diffusion. Our experimental results show that it can enhance noisy edges.

Fig. 2. A reference frame from 8 frames (240x180).

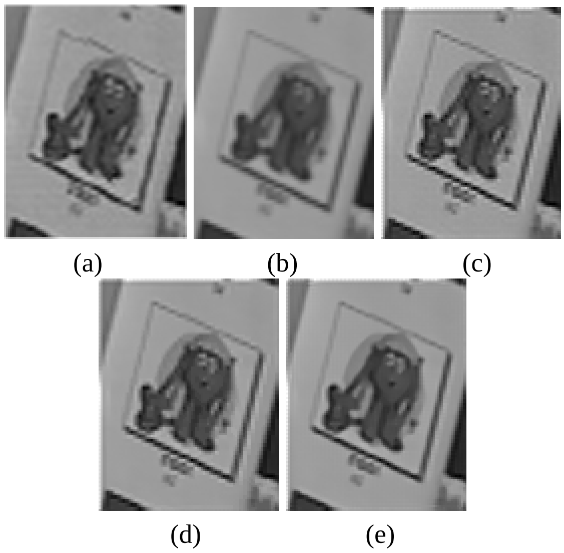

Fig. 3. Experimental result (2x2 Enlargement). (a) Bi-cubic interpolation of the reference frame, (b) Average blending, (c) Irani-Peleg estimator, (d) Edge-preserving super-resolution, (e) Edge-enhancing super-resolution ($\sigma = 0.5, \lambda = 3.0, \gamma = 0.2$).

Acknowledgement This work was supported by the Brain Korea 21 Project and we give thanks to Zomet A., from The Hebrew University for providing the video for the experiment.

8. REFERENCES

[1] Capel, D., Zisserman, A., Automated Mosaicing with Super-resolution Zoom, *Proc. International Conference on Computer Vision and Pattern Recognition*, pp. 885-891, 1998.

[2] Capel D., Zisserman A., Super-resolution Enhancement of Text Image Sequneces, *Proc. International Conference on Pattern Recognition*, pp. 600-605, 2000

[3] Elad, M., Feuer, A., Restoration of a Single Superresolution Image from Several Blurred, Noisy, and Undersampled Measured Images, *IEEE Trans. on Image Processing*(6), No. 12, December 1997, pp. 1646-1658.

[4] Irani, M., Peleg, S., Improving Resolution by Image Registration, *CVGIP: Graphical Models and Image Processing*(53), 1991, pp. 231-239.

[5] Irani, M., Peleg, S., Motion Analysis for Image Enhancement: Resolution, Occlusion, and Transparency, *Journal of Visual Communication and Image Representation*(4), 1993, pp. 324-335.

[6] Kim, H., Cohen, I., Kang E., Hong, K.S., and Medioni, G., Robust Global Registration of Dynamic Scenes, POSTECH Technical Report 2000-1, 2000.

[7] Mann, S., Picard, R.W., Virtual Bellows: Constructing High Quality Stills from Video, *Proc. International Conference on Image Processing*, 1994.

[8] Weickert, J., Nonlinear Diffusion Filtering, 15th Chapter of *Handbook of Computer Vision and Applications*, Academic Press, 1999.

[9] Zomet A., Peleg S., Efficient Super-Resolution and Applications to Mosaics, *Proc. International Conference on Pattern Recognition*, pp. 579-583, 2000